Solar Energy Materials and Solar Cells 180 (2018) 350–357

Contents lists available at ScienceDirect

Solar Energy Materials and Solar Cells

journal homepage: www.elsevier.com/locate/solmat

Materials perspectives for next-generation low-cost tandem solar cells

Teodor K. Todorov*,[1], Douglas M. Bishop*,[1], Yun Seog Lee

IBM T. J. Watson Research Center, Yorktown Heights, USA

ARTICLE INFO

Keywords:
Thin film
Photovoltaic
Perovskite
Tandem
Multijunction

ABSTRACT

Recent progress in commercial single-junction photovoltaic (PV) technologies has brought device efficiency closer to their practical limits. Module prices are dropping rapidly and solar energy has already reached grid parity in many areas. Solar module costs now constitute a small fraction of the total systems costs and to continue system cost reduction, increasing efficiency becomes even more critical. Multi-junction solar cells are the most logical path to increase PV module performance beyond 25%, but the varieties available today are still are out-performed in efficiency or cost by the main stream single-junction technologies: crystalline Si, CdTe and CIGS. Finding a solution for this problem is attracting a growing research interest. We review the latest developments in the field with particular focus on thin-film high band gap candidates such as perovskites on commercial bottom cells including silicon, CdTe and CIGS. We also review the current state of all-chalcopyrite tandems, and promising concepts using CdTe-alloys as a top cell on silicon.

1. Introduction

Thin film photovoltaics (PV) has come a long way since 1883 when Charles Fritts made the first solar cell on a metal foil coated with selenium and a thin layer of gold [1]. For more than 130 years numerous other materials and devices have been explored with the ultimate goal to make photovoltaic energy widely available. Pioneered in 1950s, crystalline silicon faced significant challenges such as an indirect band gap necessitating large quantities of ultra-pure material, and a multi-step fabrication process intense in energy consumption, technical facilities and labor. Research on direct band gap thin-film PV technologies aimed to provide a solution to these challenges and lower fabrication cost. Today grid parity is a reality, not only with thin-film front-runners CdTe and CIGS, but also with crystalline silicon that dominates the PV market [2]. The exponential reductions in PV module costs resemble the improvements in semiconductors, and although the physics of photovoltaics do not follow the size-scaling which underpins Moore's Law, the rapid technological improvements in all aspects of PV fabrication have led to a 23% reduction in cost for every doubling of manufacturing capacity [3]. This rate is faster than any other energy technology and has accelerated even more in recent years. The cost reduction stems from a variety of sources including: reduced material costs, reduced material usage, lower processing costs, and increased efficiency.

Today the costs per watt of the actual solar cells has dropped so rapidly that the cell manufacturing constitutes just a small fraction of the total PV expense, and increasingly the balance of system cost, or a commodity material such as the glass panel, drive the cost of producing solar energy [4]. Due to the shifting cost structure, increasing efficiency has become one of the most powerful levers for overall cost reduction.

Employing multiple absorbers with different band gaps in tandem or multi-junction devices is the most viable way to push the efficiency limit significantly beyond the practical limit for single-junction modules of about 25% [5]. Despite a multitude of possible material sets and structures for multi-junction solar cells, only two have made it to the market: III-V multi-junctions for concentrated light or space applications, and amorphous silicon. III-V multi-junctions currently surpass the efficiency of any other solar cell technology, however the high costs of production have relegated them to systems using optical concentration which necessitate both direct sunlight and tracking systems not suitable for building integration. Amorphous silicon is versatile, compact, and cheap allowing it to become a standard power solution for a variety of consumer products, however the efficiency of the record triple junction A-Si cell has only modestly improved in the last 30 years despite significant research and stands at 14% which is less than a typical commercial single junction multi-crystalline Si module [6]. There is an urgent need to develop efficient planar tandem PV technologies that can be implemented broadly in both utility and commercial or residential installations similar to mainstream PV today. Developing a completely new multi-junction device structure remains a possibility on the long term however a more practical and quicker solution may be instead of competing with silicon and a well-established manufacturing

* Corresponding authors.
E-mail addresses: tktodoro@us.ibm.com (T.K. Todorov), dmbishop@us.ibm.com (D.M. Bishop).
[1] Contributed equally.

http://dx.doi.org/10.1016/j.solmat.2017.07.033
Received 17 April 2017; Received in revised form 21 July 2017; Accepted 26 July 2017
Available online 24 August 2017

base, to upgrade these already large-volume technologies by integrating tandem partners on top. Taking advantage of existing infrastructure along the whole supply chain could offer a fast track for these technologies.

The largest principal distinction across all multi-junction solar cells is the way the sub-cells are interconnected. Of the multiple device architectures and interconnection schemes that can be employed for tandem solar cells [7], the only one established for commercial application is a two terminal (2-T) monolithically integrated device. This architecture has significant benefits such as requiring only one transparent conductive layer (TCL) which can be a serious source of series-resistance and light transmission losses for large-area thin-film modules. TCL losses at the module scale also help explain the large efficiency difference between lab-scale and full-scale thin-film devices. Alternative device architectures such as mechanically stacked 4-terminal, 3-terminal, and spectrum-split cells have in some cases outperformed 2-T-monolithic devices [8] however increased complexity in wiring, voltage conversion, and panel level electronics for maximum power point tracking (MPPT) for each terminal add potential costs. Due to these complications, a clear path to cost-efficient commercial application for these alternative architectures has yet to be demonstrated.

2. Common challenges for monolithic tandem integration

Beyond optimizing each individual sub-cell, there are a number of unique challenges to developing an efficient monolithic multi-junction solar cell. The two largest challenges and design criteria are: 1) proper sub-cell selection for current matching, and 2) layer process compatibility during fabrication; each of which will be described in more detail here.

– The first criteria for efficient 2-T multi-cell design is to match the current generated through each sub-cell with appropriate selection of band gaps. For a 2-T tandem cell the theoretical maximum efficiency of 46% is calculated for a band gap pairing of 0.94 eV and 1.60 eV, however only a small loss in efficiency is realized when constrained with the band gap of an established bottom cell technology such as Si or CIGS (E_g = 1.11 eV). The optimal top cell band gap for Si (or similar band gap CIGS) is approximately 1.73 eV, but a theoretical efficiency of greater than 40% can be achieved with a top cell band gap between 1.65 and 1.85 eV [9–11].

Even with the right band gap selection, to improve the efficiency of high-quality Si with a 2-T tandem junction is challenging. In 2-T devices, an efficient top cell is critical since the top cell provides a larger fraction of the total system power due to a higher voltage and the constraint of equal current imposed on both cells. The historical lack of highly efficient high-bandgap top-cells (outside of III-V growth) has made it challenging to exceed the single junction efficiency for champion silicon or CIGS.

Fig. 1 gives an example of optical distribution across a tandem structure on silicon, while Fig. 1b. shows the required efficiency for the top cell as a function of band gap to enable a 25% and 30% efficient tandem assuming a 20% efficient Si bottom cell [12].

– Process compatibility during layer fabrication is a second large restriction on the design and optimization of efficient tandems. In the case of substrate device fabrication, the bottom cell and pn-junction must withstand the maximum processing temperature of the top cell, while in the case of superstrate device the reverse must be true. One way to decouple the challenges of temperature compatibility is by bonding two complete devices [9], however the feasibility of such an approach in large scale commercial production remains to be demonstrated.

Additional challenges include providing ideal interlayers such as recombination layers or tunnel junctions to assure minimal added series resistance and parasitic optical absorption. Materials with a wide band gap, low sub-bandgap optical absorption, proper optical refractive index, proper work function, and high carrier density ($> 10^{19}$ cm^{-3}) need to be used, but detailed discussion is beyond the scope of this paper.

This review will cover the status of different material sets for multi-junction and specifically prospects for commercial tandem solar cells. The sections are broken down by material category of the top cell, first briefly highlighting III-V materials (Section 2.1), then discussing prospects for chalcogenides in Section 2.2, CdTe and II-VI alloys in Section 2.3, and perovskites in Section 2.4. In Section 2.5, a small selection of alternative and new prospective materials are highlighted.

2.1. III-V Materials as top cell in silicon devices

High band gap III-V based solar cells have been an ideal option to create high performance tandem device on conventional solar cells. However, due to the difficulties in passivating the structural defects of III-V semiconductors, so far, the fabrication process has been limited to epitaxial growth on lattice matched single crystalline substrates. Epitaxial growth of III-V on Si substrates typically results in a high density of structural defects and degraded minority lifetime due to the mismatches in lattice constant as well as thermal expansion coefficient. By incorporating GaAs/$Al_{0.22}Ga_{0.78}As$ buffer layer, a two-terminal $Al_{0.15}Ga_{0.85}As$ (E_g = 1.6 eV) / Si tandem device with 21.2% efficiency (AM0, 1 sun) has been reported [13]. Alternatively, various approaches including epitaxial lift-off and spalling have been introduced to detach

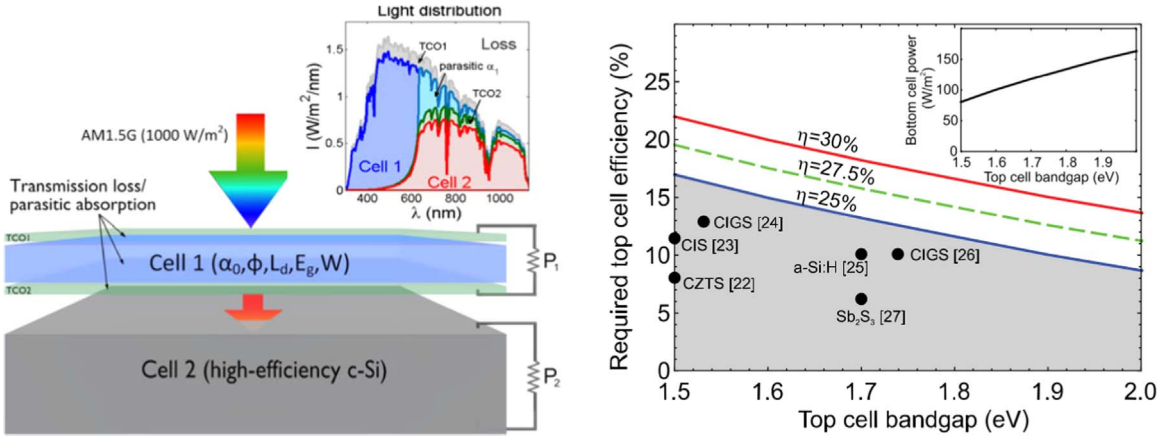

Fig. 1. Schematic representation of optical losses in a tandem solar cell. A 4-terminal example is used to show the additional loses of second TCO (a). Top cell conversion efficiency required for a top cell in a c-Si based tandem to reach 25–30% efficiency.
Reproduced with permission from [12].

epi-grown device from substrate and fabricate mechanically stacked tandem device. The approaches can be combined with chemical-mechanical polishing process to enable substrate reuse, which also reduce the cost of III-V solar cell manufacturing [14]. Mechanical stacking of $Ga_{0.5}In_{0.5}P$-based (E_g = 1.81 eV) solar cells on c-Si solar cell showed up to a 29.8% combined efficiency (AM1.5G, 1 sun) with 4-terminal configuration [15]. The limited throughput and scalability of those processes increase the module manufacturing cost significantly. Economic analysis showed that the III-V on Si tandem device can reduce installed system cost only when the area-related balance-of-system is high and the cost of III-V cells are reduced significantly [16].

2.2. Chalcogenide materials

Chalcogenide thin film solar materials including both CdTe and CIGS-related compounds have a long history of research and have continued to grow in production despite the dominance of silicon. Today, largely due to First Solar and Solar Frontier, CdTe and CIGS are respectively the first and second largest volume alternative PV materials (i.e. non-Si). Single junctions have achieved 22.6% (22.8% uncertified) for CIGS and 22.1% for CdTe, however improvements may slow as each material asymptotes towards theoretical limits [6,17,18]. Despite experimental results dating back more than 30 years, an all chalcopyrite tandem solar cell, or more broadly chalcopyrite-based top cells for tandem applications, have not yet achieved their theoretical potential [19,20]. Only a few reports have achieved an efficiency boost for the tandem structure, with a notable exception of an uncertified 23.2% CIGS-related area-mismatched 2-T tandem announced by Stion about which there are few details [21,22]. Here we lay out the band gap and material variations for CIGS and CdTe-related materials and highlight current challenges and future prospects for different tandem combinations. Chalcopyrites with perovskite top cells will be discussed in the perovskite section.

2.2.1. Chalcopyrite and CIGS-related materials

The band gap of CIS-based materials system can be modified from 1.04 eV for $CuInSe_2$ to ~1.68 eV for $CuGaSe_2$ and further increased with sulfur to 2.5 eV for $CuGaS_2$. Additional substitutions including Ag for Cu, and Al for In, allow for further ways to increase of the band gap. Despite the large number of options for band gap modification, the highest efficiency single-junction cells consistently have band gaps less than 1.2 eV. Unfortunately, in a monolithic tandem device structure, the top cell efficiency is of utmost importance and contributes the majority of the device power, and creating an efficient high-bandgap chalcopyrite CIGS-alloy has proven difficult. The top efficiencies by material class for CIGS related single-junction cells are shown in Table 1 and notable tandem device results are shown in Table 2.

Table 1
Notable efficiencies and band gaps for various CIGS-related alloys (single junction).

Selenide			
	Band gap (eV)	**Efficiency (%)**	**Reference**
$CuInSe_2$	1.04	14.5%	Abushama, 1993 [23]
$Cu(In,Ga)Se_2$ champion*	***1.09***	***22.8%***	***Rui, 2016*** [18]
$CuGaSe_2$	1.68	11.0%	Ishizuka, 2013 [24]
*contains sulfur			
Sulfide			
	Bandgap (eV)	Efficiency (%)	**Reference**
$CuInS_2$	1.5	11.4%	Siemer [25]
$Cu(In,Ga)S_2$ champion	***~1.57***	***15.5%***	***Hiroi, 2016*** [26]
CuGaS2	2.5	~1%	[27]
Alternative substitutions			
	Bandgap (eV)	Efficiency (%)	**Reference**
$(Ag,Cu)(In,Ga)Se_2$	1.2	19.9%	Thompson, 2016 [28]
$CuInAlSe_2$	1.16	16.9%	Marsillac, 2002 [29]

Table 2
Notable tandem devices with chalcopyrite (CIGS-related) top cell.

	V_{OC} (V)	Efficiency (%)	Reference
CGS / CIGS**	1.1	3.7%	[36]
CIGS / AIGS[a]	1.5	6.6%	[35]
CIGS / AIGS[a]	1.3	8.0%	[35]
CIGS / CGS[a]	1.2	7.4%	[33]
CIS / CIGS	1.08	4.4%	[34]

[a] Mechanical stack.

The key impediment for CIGS-related tandem devices is developing a highly efficient, high-bandgap transparent top cell device. While $CuGaSe_2$ with E_g = 1.67 eV is near optimal as a top cell when paired with a $CuInSe_2$ bottom cell, intrinsic defects properties and the inability create n-type doping contribute to significant interface recombination which have hindered device efficiency with the current record $CuGaSe_2$ device at 11% [24,30,31]. Recent progress on the high-bandgap pure sulfide, Cu(InGa)S_2, has enabled a 15.5% device with band gap of ~1.57 eV and a V_{OC} approaching 1 V. This sulfide progress, pioneered by Solar Frontier, has brought new interest in the area and it is likely that further improvements will be seen in the near future. Even with additional high-bandgap chalcopyrite device improvements, additional challenges will need to be met to enable the promise of chalcopyrite tandems.

2.2.2. Chalcopyrite/chalcopyrite tandems

The largest challenge for a chalcopyrite/chalcopyrite tandem is the processing temperature compatibility for the top and bottom layers. Traditionally diffusion occurs in the pn-heterojunction, and at temperatures above ~200°C, the device performance quickly degrades. This requirement severely limits the processing temperature of the second junction. Due to the need for high processing temperatures (450–600°C) to obtain high quality chalcopyrite, previous tandems have been fabricated with mechanical stacking to allow each cell to be processed independently followed by mechanically connecting the top and bottom junction. It is not yet clear if this approach, and in particular the mating of top and bottom junctions can be made commercially viable, but it is likely that this will be the continued direction for all-chalcopyrite tandems in research. Ideally, to eliminate physical wiring between top and bottom junction and to avoid an additional encapsulation layer, the top cell would be processed in the superstrate fashion, while the bottom cell would be processed in the traditional substrate fashion enabling a glass/glass structure. A 4-T structure may be easier to build with a mechanical stack than a monolithic-2-T, although a transparent back contact for the top cell is required. The need for a transparent back contact, again encourages a superstrate design due to the degradation of the TCO at the processing temperatures required for the CIGS-layer. The challenges in superstrate fabrication are highlighted by Heinemann et al. [32].

To date, due to the aforementioned challenges, very few tandems exist with CIGS-based top cells and the most successful examples have used mechanical stacking [33–35]. Despite some momentum on the pure sulfide system, most research will forgo chalcopyrite-only monolithic tandems, in favor of continued mechanical stacking. High-bandgap CIGS on Si, which can withstand high temperatures, is another combination of potential promise, however the impressive, highly efficient, and high-bandgap perovskites will likely continue to dominate the tandem efficiency chart. It is likely that most CIGS tandem research will continue to pair CIGS bottom cell with perovskite top cell. The low processing temperatures of perovskites enable monolithic integration, and the efficiency of CIGS across the low-bandgap range (~1.05 − 1.2 eV), will help enable efficient 2-T designs, as will be discussed in the perovskite section.

CZTS is a related material set with similar range of band gap

flexibility due to various anion and cation substitutions, however with maximum efficiency at 12.6% [37] and a similar set of daunting barriers (i.e. junction temperature processing and superstrate growth), CIGS is clearly the more relevant and more mature choice for high efficiency tandems for the foreseeable future.

2.3. CdTe and II-VI alloys

CdTe, with a band gap of 1.48 eV, is less associated with band gap variation due to typical fabrication near stoichiometry, however CdTe-solid solutions have the potential to significantly expand the band gap range. HgTe is a semi-metal (E_g ~0 eV) and partial substitution for $Cd_{1-x}Hg_xTe$ would allow the band gap to be lowered to below 1 eV as required for multi-junctions. The low band gap and tailorable well-behaved solid solution of CdHgTe has led to its successful use in infrared detectors. Zn and Mg, on the other hand, can increase the band gap of CdTe, with maximums of 2.26 eV for ZnTe, and 3.5 eV for MgTe. $Cd_{1-x}Zn_xTe$ has been commercialized for x-ray and gamma-ray detectors while $Mg_xCd_{1-x}Te$ has shown significant promise as a passivation layer in a double heterostructures and has recently been investigated for tandems. It is worth noting the record CdTe solar cells have an effective of band gap ~90 meV below the pure material achieved by alloying with small quantities of Se in the junction. The band gap narrowing occurs due to the bowing of the band gap in the alloy system which reaches a max of 1.74 eV for CdSe. A summary of the champion device results for single junction CdTe and related alloys is listed in Table 3.

2.3.1. CdTe related tandems

The band gap for CdTe is naturally low for a top cell and high for a bottom cell, and therefore outside the optimal range for a tandem device. The non-optimal band gap match is demonstrated by recent modeling. Using QE data from previous record cells, a 21.5% CdTe cell stacked on a 25.6% Si cell, could increase only to a maximum of 27.3% in a monolithic tandem if no additional stacking losses are assumed [9]. Prospects for tandem performance increase significantly if the band gap of the top cell can be increased to near the optimal, which for Si is slightly above 1.7 eV. CdZnTe and CdMgTe are attractive candidate to achieve this goal [42–44]. As listed in Table 4, the highest efficiency CdTe-related tandem to date was achieved by epitaxially grown CdZnTe on Si which achieved 16.8% with a notable V_{OC} of 1.75 eV [45].

For CdTe utilized as a bottom cell, a top cell band gap of ~2.0 eV is expected to be optimal with theoretical efficiencies approaching 40% [46]. This high top-cell band gap requirement is relaxed significantly for 4-terminal design, however this adds cost and complication to the fabrication. An alternative approach is to lower of the band gap of CdTe cell with Hg or other elements to approach the ideal range of 1.1–1.2 eV for the bottom and 1.7–1.8 eV top cell. With the progress in epitaxial growth in CdTe related alloy systems [38], an all CdTe based tandem seems an attractive prospect for future development. Such a concept was demonstrated with limited efficiency in the past [47].

Few complete tandem devices have been published for CdTe-based materials and they are listed in Table 4. As mentioned, the most exceptional result was an epitaxially grown Si/CdZnTe tandem achieved 16.8% and high V_{OC} [45]. Polycrystalline CdTe tandems have yet to reach similar maturity with the best efficiency coming from a 4-T mechanically stacked CIS/CdTe which achieved 15.3% combined. This design however would not be possible as a 2-T device due to non-optimal band gap pairing causing poor current matching [48].

Table 4
Notable CdTe-related tandem devices.

	V_{OC} (V)	Efficiency	Reference
Si / CdZnTe	1.75	16.8%	[39] Carmody et al., 2010
CdHgTe / CdTe	0.99	1.2%	[47] Wang et al., 2005
CIS / CdTe	1.02	3.0%	[19] Meakin et al., 1986
CIS / CdTe (4-T)		15.3%	[48] Wu et al. 2006

The future prospects for CIGS/CdTe will likely continue to require a mechanical stacked junction to avoid the challenges of processing temperature affecting the CIGS junction. Bandgap matching will continue to be a challenge until high-bandgap (1.7–1.8 eV) CdTe based top cells can be demonstrated. One advantage for CdTe as a top cell, is the default superstrate fabrication is naturally suited as a top cell in mechanically stacked junctions. An epitaxial all CdTe-alloy tandem also seems a feasible and attractive area for future research.

The most promising area for near term applications of chalcogenide-based tandems is likely to be high-bandgap CdTe alloys on a Si bottom cell. Silicon is efficient, an appropriate band gap, withstands high processing temperatures, and can enable epitaxial growth which can be beneficial for CdTe. Recent breakthroughs in CdTe and CdMgTe lifetime in epitaxial heterostructures, and progress on doping suggest that Si/CdMgTe and Si/CdZnTe tandem devices are both practical, and extremely promising.

2.4. Perovskite tandems

Halide perovskites have recently achieved the most rapid efficiency growth of any photovoltaic material, reaching over 22% in just a few years – on par with long-standing veterans CIGS and CdTe [6]. What makes these devices particularly attractive for tandem applications are their tunable optoelectronic properties and processing temperatures below 150°C - lower than any other high-performance absorber [49]. The first high-efficiency devices were made with $CH_3NH_3PbI_3$ having a relatively high band gap of 1.55 eV [49], which can be readily tuned across the range of interest for PV applications with multiple cationic or anionic substitutions. For example the band gap can be decreased to approximately 1 eV by substituting Pb with Sn [50] and increased to 2.2 eV by substituting I with Br [51]. Other substitutions such as Cs and formamidinium have demonstrated enhancement in thermal and overall device stability [52,53]. Some examples of high performance devices with significantly shifted band gaps include an 11.5% efficiency achieved at 2 eV with $Cs_{0.15}FA_{0.85}Pb(Br_{0.7}I_{0.3})_3$ [54], 17.6% at 1.25 eV and 14.8% at 1.2 eV with $FA_{0.83}Cs_{0.17}Pb(I_{0.5}Br_{0.5})_3$ [53]. A summary of notable single and tandem junction perovskites is shown in Table 5. While the outstanding performance of perovskites at high band gap makes them compatible with commercial low band gap PV technologies, the ongoing optimization of low band gap devices significantly expands the possibilities for an all-perovskite multi-junction [55,56].

Table 3
Notable device efficiency of CdTe and related alloys.

	Band gap (eV)	V_{OC} (V)	Efficiency (%)	Reference
CdTe (polycrystalline)	1.4	0.887	22.1	[6]
CdTe (single crystal)	1.48	1.09	18.5	[38]
CdZnTe (single crystal)	1.8	1.3	16	[39]
CdZnTe	1.6	0.78	11.5	[40]
CdHg(0.1)Te	1.3	0.62	10.6	[41]

Table 5
Examples of high-performance perovskite devices and tandems.

Single junction				
Device type	**Band gap (eV)**	**Efficiency (%)**	**Fabrication sequence**	**Reference**
Perovskite	1.49	22.1	Straight	[6]
Perovskite	~1.58	20.1	Inverted	[73]
Perovskite(Low E_g)	1.25	17.6	Inverted	[74]
Perovskite(High E_g)	2.0	11.0	Inverted	[54]

Tandem junction			
Device type	**Efficiency (%)**	**Fabrication sequence**	**Reference**
All-perovskite stacked	20.3	Inverted	[72]
All-perovskite monolithic	17.0	Inverted	[72]
All-perovskite monolithic	10.8	Straight + Inverted	[71]
CIGS- 2-T monolithic	10.9	Inverted	[75]
CIGS- 2-T stacked	18.5	Straight	[69]
CIGS- 4-T stacked	20.7	Straight	[76]
CIGS-4-T stacked	22.1	Inverted	[77]
Si- 4-T stacked	25.2	Straight	[64]
Si- 4-T spectrum split	28.0	Straight	[8]
Si- 2-T monolithic	19.9	Straight	[65]
Si −2-T monolithic	23.6	Inverted	[70]

There are two general fabrication orders for the perovskite solar cell, often referred to as “straight” and “inverted” depending on the order of layer deposition. These are not to be confused with “substrate” and “superstrate” as both have been operated in either configuration, the most common one being superstrate taking advantage of pre-deposited TCL (conductive oxide) on glass. Depositing TCL on a perovskite-containing stacks is challenging due to their low thermal and chemical stability. Standard sputtering or chemical vapor deposition (CVD) of conductive oxides easily cause plasma and/or thermal damage to the sensitive perovskite layers and interfaces. This poses significant processing challenges for tandem integration as most perovskite tandems require depositing either another solar cell or some form of TCL on a perovskite-containing stack. In early works above standard techniques were avoided completely by use of alternative TCL such as Ag nanowires [57] or thin semitransparent evaporated metals [58,59]. For higher performance TCL soft sputtering conditions were later developed, usually in combination with protective non-sputtered oxides such as MoO_3 [60,61], nanoparticle layers [62] or low-temperature ALD [63].

2.4.1. Straight configuration

The “straight” configurations is the most common fabrication order, and its evolution can be traced back to the dye-sensitized solar cell. Fabrication begins with depositing n-type TiO_2 layer that is often a combination of dense hole blocking and mesoporous layer on FTO-coated glass, followed by the perovskite layer, hole-selective layer and back contact [49]. This configuration is the most thoroughly optimized and has achieved the current 22.1% efficiency record [6]. It is also used in the highest performance 4-terminal tandems with silicon including 25.2% stacked [64] and 28% spectrum split device [8]. However, 2-terminal monolithic integration of this structure with the most common bottom cells including CIGS and Si is not straightforward due to inability of the perovskite to withstand the temperature processing of the bottom sub-cell. Two possible solutions include creating each sub-cell separately and mechanically bonding with a transparent conductive epoxy, or using a bottom sub-cell with low temperature requirements such as another perovskite.

Similarly, reversing the fabrication order and building a tandem on top of a bottom junction in the substrate fashion also has challenges. In this case, the n-type layer, which is TiO_2 for the highest-performance devices, typically requires annealing at temperatures in excess of 450°C that could cause degradation to most bottom cells. Alternative low-temperature n-layers or electron-selective layers such as SnO_2 have produced tandems with 19.9% (18.1% stabilized) efficiency [65], while ZnO in combination with PCBM have reached 20.5% [66]. Another possibility is to reverse the pn-junction order for both top and bottom cells allowing the n-type TiO_2 to be deposited before the p-type perovskite. Although this means the pn-junction is at the bottom of the perovskite and requires an n-type Si absorber, it has demonstrated a respectable 13.8% efficiency in one of the earliest reports on monolithic perovskite tandems [57].

2.4.2. Inverted configuration

The “inverted” perovskite single junction cell configuration where the fabrication process starts with the p-side has also yielded high-efficiency devices, close to 20% [67]. This configuration is suitable for direct monolithic integration on top of most p-type substrate solar cells as it can be fabricated at low temperature (<150°C) without inflicting thermal damage to the bottom stack. Commonly used materials for the hole-transport layer include PEDOT and NiO. The top n-type layer is usually a fullerene derivative such as PCBM, either alone or in combination with other layers such as bathocuproine (BCP), C60 or LiF to improve the band alignment and charge injection [68]. The inverted configuration was used for the first demonstration of a monolithic perovskite tandem paired with a CZTS bottom cell [58], as well as the currently highest efficiency monolithic tandems with both CIGS [69] and silicon [70]. The structure of the record 23.6% efficient 2-T silicon-perovskite solar cell [70] is shown in Fig. 2. The record was achieved by merging state-of the art developments across the fields of both devices to enable at the same time excellent light management and processing conditions for a high-efficiency tandem with enhanced stability. The Si solar cell was optimized for the infrared spectrum and patterned only on the back providing smooth interface for perovskite deposition. For the perovskite cell, a robust NiOx hole selective layer was used instead of PEDOT to achieve higher voltage and stability. The perovskite absorber was designed with composition $Cs_{0.17}FA_{0.83}Pb(Br_{0.17}I_{0.83})3$ for improved stability due to Cs and formamidinium substitution and increased band gap via Br substitution (1.63 eV). Lastly the SnO_2-ZnO buffer on top of the PCBM layer provided both efficient electron extraction, minimal parasitic absorption and protection against the sputtered ITO layer. The resulting device exhibited remarkable stability during 1000 h damp-heat test [70].

Recent advances in charge-recombination layers with optimized mild processing conditions have enabled pure perovskite-perovskite tandem solar cells initially yielding only 7% [71], more recently 10.8% [71], and now achieving 17% in monolithic and 20.4% with an inverted configuration [72].

Given the new state of the perovskite field and the extremely rapid progress over the past few years, future prospects for further efficiency gains seem very bright. Significant challenges still remain, primarily improving stability and reducing potential toxicity by using non-heavy metals to replace Pb. Despite these obstacles, research continues to progress rapidly and prospects for commercial applications are already being pursued.

2.5. Other high band gap materials for future tandem solar cells

The search for the ideal high band gap materials for monolithic tandem integration should not be limited to above examples. Both the discovery of new materials as well as re-examining existing ones with the latest device engineering approaches could bring interesting candidates for future planar tandem applications. Exhaustive review of these is beyond the scope of this work however we will give two

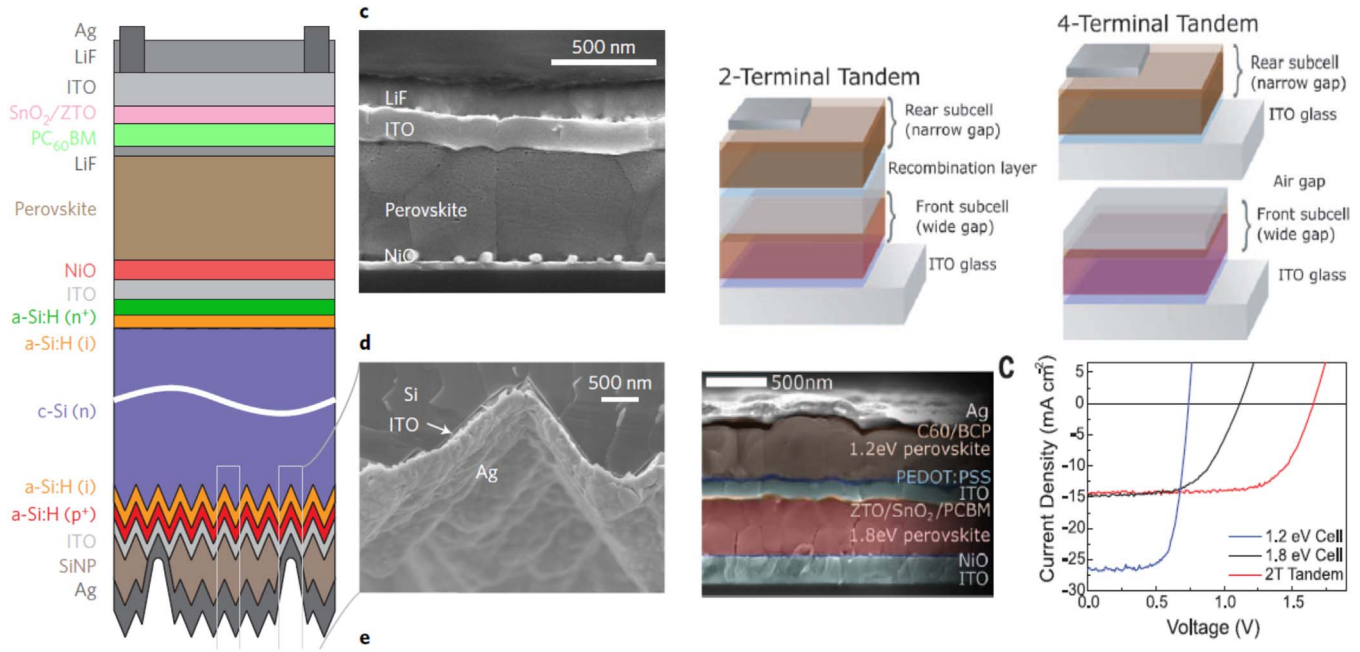

Fig. 2. Monolithic Si-perovskite tandem with 23.6% efficiency. Reproduced with permission from [70] and all-perovskite 2-terminal tandem. Reproduced with permission from [72].

examples of recent progress with two historic materials that can meet the processing requirements for tandem integration.

Copper(I) oxide (Cu_2O) the oldest semiconductor material, has a high band gap of 1.9–2.1 eV with a theoretical maximum efficiency of ~20% [78]. High quality Cu_2O can be prepared by annealing copper foil at 900 – 1100°C with controlled temperature and oxygen partial pressure profile to prevent Cu or CuO phase formation [79]. Low-temperature processes more interesting for monolithic integration such as electrochemical deposition, sputtering, chemical vapor deposition have been also used to grow Cu_2O thin films [78,80,81]. Since Cu_2O shows intrinsic p-type conductivity and n-type doping is typically challenging, the most common approach to create solar cell device is a heterojunction with n-type wide band gap materials [82,83,84]. Current bottlenecks for Cu_2O-based solar cell device include band alignment at the heterojunction and bulk/interface defect control. However recent developments with ZnO:Al/Zn_xGe_yO/Cu_2O heterojunction solar cells have reached up to 8.1% efficiency [85].

Selenium, which was the first PV absorber, also has potential for tandem applications due to its high band gap of >1.9 eV and low processing temperature of less than 200°C. Selenium efficiency plateaued at 5% in 1985 with little attention, until recent research demonstrated an improved efficiency of 6.5% and a path towards even higher efficiencies [86]. The system is stable, non-toxic, low cost, and very simple to fabricate making it an attractive material for further investigation.

3. Conclusions

Improving module efficiency to 25% and beyond while maintaining low cost, lies at the center of continuing PV growth and system cost reduction. Given the commercial success and expanding volume of silicon, as well as CIGS and CdTe, the most likely path to >25% modules will be tandem solar cells based on current established technologies. In this paper, we have tried to survey the prospects and current status of the most common material sets that could be utilized as a tandem top cell. We will summarize some of the key findings here. III-V materials continue to hold record efficiencies for multi-junctions, and recently have shown progress with growth and integration with silicon bottom cells, but it is not yet clear if cost barriers can be reduced enough to enable mass production. Chalcopyrite and CIGS related materials can be tailored to achieve the desired band gap range for both bottom and top cells, however, despite recent progress for high voltage sulfur-containing devices, limiting efficiencies for high band gap devices and extremely challenging process compatibility for monolithic growth are large barriers to successful all-chalcopyrite tandems and chalcopyrite top cells in general. CIGS devices have a more likely role as high efficiency bottom cells for perovskite tandems. CdTe similarly can similarly achieve a band gap range theoretically suitable for top or bottom cells through alloying. Recent improvement in understanding CdTe defect physics, doping, and lifetime, as well as high band gap hetero-structures utilizing CdMgTe suggest very promising potential for CdTe top cells grown on Si. The fastest growing research area for tandems has been perovskites. Their exceptional efficiencies and high band-gaps, coupled with low fabrication temperatures make them compatible for monolithic integration with both silicon and CIGS. It is likely this research area will continue to change rapidly and despite the need for improved stability and reduced toxicity, record efficiencies and new commercial ventures are bound to be seen.

References

[1] C.E. Fritts, On a new form of selenium cell, and some electrical discoveries made by its use, Am. J. Sci. 3–26 (156) (1883) 465–472.
[2] M.A. Green, Commercial progress and challenges for photovoltaics, Nat. Energy 1 (1) (2016) 15015.
[3] E.S. Rubin, I.M.L. Azevedo, P. Jaramillo, S. Yeh, A review of learning rates for electricity supply technologies, Energy Policy 86 (2015) 198–218.
[4] T. Installed, D.M. Lbnl, S. Cates, N. Disanti, R. Widiss, Tracking the Sun IX, 2016.
[5] M.A. Green, Commercial progress and challenges for photovoltaics, Nat. Energy 1 (1) (2016) 15015.
[6] M.A. Green, K. Emery, Y. Hishikawa, W. Warta, E.D. Dunlop, D.H. Levi, A.W.Y. Ho-Baillie, Solar cell efficiency tables (version 49), Prog. Photovolt. Res. Appl. 25 (1) (2017) 3–13.
[7] T.K. Todorov, O. Gunawan, S. Guha, A road towards 25% efficiency and beyond: perovskite tandem solar cells, Mol. Syst. Des. Eng. 1 (2016) 370–376.
[8] H. Uzu, M. Ichikawa, M. Hino, K. Nakano, T. Meguro, J.L. Hernández, H.S. Kim, N.G. Park, K. Yamamoto, High efficiency solar cells combining a perovskite and a silicon heterojunction solar cells via an optical splitting system, Appl. Phys. Lett. 106 (1) (2015) 0–4.
[9] Z. (Jason), Yu, M. Leilaeioun, Z. Holman, Selecting tandem partners for silicon solar cells, Nat. Energy 1 (September) (2016) 16137.
[10] S.P. Bremner, C. Yi, I. Almansouri, A. Ho-Baillie, M.A. Green, Optimum band gap combinations to make best use of new photovoltaic materials, Sol. Energy 135 (2016) 750–757.
[11] S.P. Bremner, M.Y. Levy, C.B. Honsberg, Analysis of tandem solar cell efficiencies

under AM1.5G spectrum using a rapid flux calculation method, Prog. Photovolt. Res. Appl. 16 (3) (2008) 225–233.
[12] T.P. White, N.N. Lal, K.R. Catchpole, Tandem solar cells based on high-efficiency c-Si bottom cells: top cell requirements for >30% efficiency, IEEE J. Photovolt. 4 (1) (2014) 208–214.
[13] M. Umeno, T. Soga, K. Baskar, T. Jimbo, Heteroepitaxial technologies on Si for high-efficiency solar cells, Sol. Energy Mater. Sol. Cells 50 (1–4) (1998) 203–212.
[14] J.S. Ward, T. Remo, K. Horowitz, M. Woodhouse, B. Sopori, K. VanSant, P. Basore, Techno-economic analysis of three different substrate removal and reuse strategies for III-V solar cells, Prog. Photovolt. Res. Appl. 24 (9) (2016) 1284–1292.
[15] W. Efficiency, S. Essig, M.A. Steiner, C. Alleb, J.F. Geisz, B. Paviet-salomon, S. Ward, A. Descoeudres, V. Lasalvia, L. Barraud, N. Badel, A. Faes, J. Levrat, M. Despeisse, C. Ballif, P. Stradins, D.L. Young, Realization of GaInP / Si dual-junction solar cells, IEEE J. Photovolt. 6 (4) (2016) 1012–1019.
[16] D.C. Bobela, L. Gedvilas, M. Woodhouse, K.A.W. Horowitz, P.A. Basore, Economic competitiveness of III-V on silicon tandem one-sun photovoltaic solar modules in favorable future scenarios, Prog. Photovolt. Res. Appl. 25 (1) (2017) 41–48.
[17] P. Jackson, R. Wuerz, D. Hariskos, E. Lotter, W. Witte, M. Powalla, Effects of heavy alkali elements in Cu(In,Ga)Se 2 solar cells with efficiencies up to 22.6%, Phys. Status Solidi - Rapid Res. Lett. 4 (8) (. 2016) 1–4.
[18] K. Rui, Y. Takeshi, A. Shunsuke, H. Atsushi, F.T. Kong, K. Takuya, S. Hiroki, New World Record Cu(In,Ga)(Se,Se,Se,S)2 Thin Film Solar Cell Efficiency Beyond 22%, in: Proceedings of the 2016 IEEE 43th Photovolt. Spec. Conference PVSC 2016 Portland(OR) USA, June 2016., pp. 3–7, 2016.
[19] J.D. Meakin, R.W. Birkmire, L.C. Dinetta, P.G. Lasswell, J.E. Phillips, Thin film tandem solar cells based on CuInSe2, Sol. Cells 16 (1986) 447–455.
[20] M. Schmid, R. Klenk, M.C. Lux-Steiner, Quantitative analysis of cell transparency and its implications for the design of chalcopyrite-based tandems, Sol. Energy Mater. Sol. Cells 93 (6–7) (. 2009) 874–878.
[21] "Stion Demonstrates 23.2% Efficiency Thin Film With Simply Better Tandem Technology."
[22] G. Cheek, F. Yang, H. Lee, Thin film PV: moving at the speed of solar, Conf. Rec. IEEE Photovolt. Spec. Conf. 2 (2013) 3407–3410.
[23] J.A.M. AbuShama, S. Johnston, T. Moriarty, G. Teeter, K. Ramanathan, R. Noufi, Properties of ZnO/CdS/CuInSe2 solar cells with improved performance, Prog. Photovolt. Res. Appl. 12 (1) (2004) 39–45.
[24] S. Ishizuka, A. Yamada, P.J. Fons, H. Shibata, S. Niki, Impact of a binary Ga2Se3 precursor on ternary CuGaSe2 thin-film and solar cell device properties, Appl. Phys. Lett. 103 (14) (2013) 3–8.
[25] K. Siemer, J. Klaer, I. Luck, J. Bruns, R. Klenk, D. Bräunig, Efficient CuInS2 solar cells from a rapid thermal process (RTP), Sol. Energy Mater. Sol. Cells 67 (1–4) (2001) 159–166.
[26] H. Hiroi, Y. Iwata, S. Adachi, H. Sugimoto, A. Yamada, New World-Record Efficiency for Pure-Sulfide Cu (In, Ga) S2 Thin-Film Solar Cell With Cd-Free Buffer Layer via KCN-Free Process, pp. 1–4, 2016.
[27] K. Tanaka, K. Ishii, S. Matsuda, Y. Hasegawa, K. Sato, Optical characterization of deep levels in single crystals of $CuGaS_2$ grown by chemical vapor transport, Jpn. J. Appl. Phys. 28 (1) (1989) 12–15.
[28] C.P. Thompson, L. Chen, W.N. Shafarman, J. Lee, S. Fields, R.W. Birkmire, Bandgap gradients in (Ag,Cu)(In,Ga)Se2 thin film solar cells deposited by three-stage co-evaporation, in: Proceedings of the 2015 IEEE Proceedings of the 42nd Photovoltaic Specialist Conference, PVSC 2015, 2015.
[29] S. Marsillac, P.D. Paulson, M.W. Haimbodi, R.W. Birkmire, W.N. Shafarman, High-efficiency solar cells based on Cu(InAl)Se2 thin films, Appl. Phys. Lett. 81 (7) (2002) 1350–1352.
[30] J.V. Li, S. Grover, M.A. Contreras, K. Ramanathan, D. Kuciauskas, R. Noufi, A recombination analysis of Cu(In,Ga)Se2 solar cells with low and high Ga compositions, Sol. Energy Mater. Sol. Cells 124 (2014) 143–149.
[31] M.A. Contreras, L.M. Mansfield, B. Egaas, J. Li, M. Romero, R. Noufi, E. Rudiger-Voigt, W. Mannstadt, Wide bandgap Cu(In,Ga)Se 2 solar cells with improved energy conversion efficiency, Prog. Photovolt. Res. Appl. 20 (7) (2012) 843–850.
[32] M.D. Heinemann, V. Efimova, R. Klenk, B. Hoepfner, M. Wollgarten, T. Unold, H.-W. Schock, C.A. Kaufmann, Cu(In,Ga)Se 2 superstrate solar cells: prospects and limitations, Prog. Photovolt. Res. Appl. 23 (10) (2015) 1228–1237.
[33] S. Nishiwaki, S. Siebentritt, P. Walk, M.C. Lux-Steiner, A stacked chalcopyrite thin-film tandem solar cell with 1.2 V open-circuit voltage, Prog. Photovolt. Res. Appl. 11 (4) (2003) 243–248.
[34] R. Kaigawa, K. Funahashi, R. Fujie, T. Wada, S. Merdes, R. Caballero, R. Klenk, Tandem solar cells with Cu(In,Ga)S2 top cells on ZnO coated substrates, Sol. Energy Mater. Sol. Cells 94 (11) (2010) 1880–1883.
[35] T. Nakada, S. Kijima, Y. Kuromiya, R. Arai, Y. Ishii, N. Kawamura, H. Ishizaki, N. Yamada, Chalcopyrite thin-film tandem solar cells with 1.5 V open-circuit-voltage, in: Proceedings of the Conference Record 2006 IEEE Proceedings of the 4th World Conference Photovoltaic Energy Conversion, WCPEC-4, vol. 1, pp. 400–403, 2007.
[36] D.L. Young, J. Abushama, R. Noufi, X. Li, J. Keane, T.A. Gessert, J.S. Ward, M. Contreras, T.J. Coutts. A new thin-film CuGaSe2/Cu (In, Ga) Se2 bifacial, tandem solar cell with both junctions formed simultaneously preprint, in: Proceedings of the Records of Twenty-Ninth IEEE Photovolatic Special Conference, 2002, pp. 608–611.
[37] W. Wang, M.T. Winkler, O. Gunawan, T. Gokmen, T.K. Todorov, Y. Zhu, D.B. Mitzi, Device characteristics of CZTSSe thin-film solar cells with 12.6% efficiency, Adv. Energy Mater. 4 (7) (2014) 1301465.
[38] J.J. Becker, M. Boccard, C.M. Campbell, Y. Zhao, M. Lassise, Z.C. Holman, Y. Zhang, Loss analysis of monocrystalline CdTe solar cells with 20% active-area efficiency, J. Photovolt. (2017) 1–6.
[39] M. Carmody, S. Mallick, J. Margetis, R. Kodama, T. Biegala, D. Xu, P. Bechmann, J.W. Garland, S. Sivananthan, Single-crystal II-VI on Si single-junction and tandem solar cells, Appl. Phys. Lett. 96 (15) (2010).
[40] B.E. McCandless, R.W. Birkmire, Cd1-xZnxTe solar cells with 1.6 eV band gap, Conf. Rec. IEEE Photovolt. Spec. Conf. (2005) 398–401.
[41] B.M. Basol, Electrodeposited CdTe and HgCdTe solar cells, Sol. Cells 23 (1–2) (1988) 69–88.
[42] R. Dhere, T. Gessert, J. Zhou, S. Asher, J. Pankow, H. Moutinho, Investigation of CdZnTe for thin-film tandem solar cell applications, in: Proceedings of the Material Research Society Symposium, vol. 763, no. April, 2003, pp. 409–414.
[43] S. Liu, X.-H. Zhao, C.M. Campbell, M.J. DiNezza, Y. Zhao, Y.-H. Zhang, Minority carrier lifetime of lattice-matched CdZnTe alloy grown on InSb substrates using molecular beam epitaxy, J. Vac. Sci. Technol. B, Nanotechnol. Microelectron. Mater. Process. Meas. Phenom. 33 (1) (2015) 11207.
[44] C.M. Campbell, Y. Zhao, E. Suarez, M. Boccard, X. Zhao, Z. He, P.T. Webster, M.B. Lassise, S. Johnson, Z. Holman, Y. Zhang, 1.7 eV MgCdTe double-hetero-structure solar cells for Tandem Device Applications, IEEE J. Photovolt. (2016) 3–6.
[45] S. Sivananthan, J.W. Garland, and M.W. Carmody, Multijunction single-crystal CdTe-based solar cells: opportunities and challenges, vol. 7683, p. 76830N, 2010.
[46] S. Rühle, The detailed balance limit of perovskite/silicon and perovskite/CdTe tandem solar cells, Phys. Status Solidi 1600955 (2017) 1600955.
[47] S.L. Wang, J. Drayton, V. Parikh, A. Vasko, A. Gupta, A.D. Compaan, Preparation and characterization of monolithic HgCdTe/CdTe tandem cells, in: Proceedings of the Material Research Symposium, vol. 836, 2005, pp. 1–6.
[48] X. Wu, J. Zhou, A. Duda, J.C. Keane, T.A. Gessert, Y. Yan, R. Noufi, 13.9%-efficient CdTe polycrystalline thin-film solar cells with an infrared transmission of ~50%, Prog. Photovolt. Res. Appl. 14 (6) (2006) 471–483.
[49] H.J. Snaith, Perovskites: the emergence of a new era for low-cost, high-efficiency solar cells, J. Phys. Chem. Lett. 4 (2013) 3623–3630.
[50] F. Hao, C.C. Stoumpos, R.P.H. Chang, M.G. Kanatzidis, Anomalous band gap behavior in mixed Sn and Pb perovskites enables broadening of absorption spectrum in solar cells, J. Am. Chem. Soc. 136 (22) (2014) 8094–8099.
[51] B. Suarez, V. Gonzalez-Pedro, T.S. Ripolles, R.S. Sanchez, L. Otero, I. Mora-Sero, Supporting information: recombination study of combined halides (Cl, Br, I) perovskite solar cells, J. Phys. Chem. Lett. 5 (10) (2014) 1628–1635.
[52] R.J. Sutton, G.E. Eperon, L. Miranda, E.S. Parrott, B.A. Kamino, J.B. Patel, M.T. Hörantner, M.B. Johnston, A.A. Haghighirad, D.T. Moore, H.J. Snaith, Bandgap-tunable cesium lead halide perovskites with high thermal stability for efficient solar cells, Adv. Energy Mater. 6 (8) (2016) 1502458.
[53] G.E. Eperon, T. Leijtens, K.A. Bush, T. Green, J.T.-W. Wang, D.P. McMeekin, G. Volonakis, R.L. Milot, D.J. Slotcavage, R. Belisle, J.B. Patel, E.S. Parrott, R.J. Sutton, W. Ma, F. Moghadam, B. Conings, A. Babayigit, H. Boyen, F. Giustino, L.M. Herz, M.B. Johnston, M.D. McGehee, H.J. Snaith, Perovskite-perovskite tandem photovoltaics with ideal bandgaps, ArXiv 9717 (2016) 1–10.
[54] D. Forgács, D. Pérez-del-Rey, J. Ávila, C. Momblona, L. Gil-Escrig, B. Dänekamp, M. Sessolo, H.J. Bolink, Efficient wide band gap double cation – double halide perovskite solar cells, J. Mater. Chem. A (2017).
[55] J.H. Heo, S.H. Im, $CH_3NH_3PbBr_3$-$CH_3NH_3PbI_3$ perovskite-perovskite tandem solar cells with exceeding 2.2 V open circuit voltage, Adv. Mater. (2016) 5121–5125.
[56] F. Jiang, T. Liu, B. Luo, J. Tong, F. Qin, S. Xiong, Z. Li, Y. Zhou, Two-terminal perovskite/perovskite tandem solar cell, J. Mater. Chem. A 0 (2015) 1–6.
[57] J.P. Mailoa, C.D. Bailie, E.C. Johlin, E.T. Hoke, A.J. Akey, W.H. Nguyen, M.D. McGehee, T. Buonassisi, A 2-terminal perovskite/silicon multijunction solar cell enabled by a silicon tunnel junction, Appl. Phys. Lett. 106 (12) (2015).
[58] T. Todorov, T. Gershon, O. Gunawan, C. Sturdevant, S. Guha, Perovskite-kesterite monolithic tandem solar cells with high open-circuit voltage, Appl. Phys. Lett. 105 (17) (2014).
[59] T.K. Todorov, T.S. Gershon, O. Gunawan, Y.S. Lee, C. Sturdevant, L.-Y.Y. Chang, S. Guha, Monolithic perovskite-CIGS tandem solar cells via in situ band gap engineering, Adv. Energy Mater. 5 (23) (2015).
[60] F. Fu, T. Feurer, T. Jäger, E. Avancini, B. Bissig, S. Yoon, S. Buecheler, A.N. Tiwari, Low-temperature-processed efficient semi-transparent planar perovskite solar cells for bifacial and tandem applications, Nat. Commun. 6 (2015) 8932.
[61] J. Werner, C.H. Weng, A. Walter, L. Fesquet, J.P. Seif, S. De Wolf, B. Niesen, C. Ballif, Efficient monolithic perovskite/silicon tandem solar cell with cell area >1 cm^2, J. Phys. Chem. Lett. 7 (1) (2016) 161–166.
[62] B. Chen, Y. Bai, Z. Yu, T. Li, X. Zheng, Q. Dong, L. Shen, M. Boccard, A. Gruverman, Z. Holman, J. Huang, Efficient semitransparent perovskite solar cells for 23.0%-efficiency perovskite/silicon four-terminal tandem cells, Adv. Energy Mater. 6 (19) (2016) 0–7.
[63] K.A. Bush, A.F. Palmstrom, Z.J. Yu, M. Boccard, R. Cheacharoen, J.P. Mailoa, D.P. Mcmeekin, R.L.Z. Hoye, C.D. Bailie, T. Leijtens, I.M. Peters, M.C. Minichetti, N. Rolston, R. Prasanna, S. Sofia, D. Harwood, W. Ma, F. Moghadam, H.J. Snaith, T. Buonassisi, Z.C. Holman, S.F. Bent, M.D. Mcgehee, Tandem Sol. Cells Improv. Stab. (2017) 1–7.
[64] D.P. McMeekin, G. Sadoughi, W. Rehman, G.E. Eperon, M. Saliba, M.T. Horantner, A. Haghighirad, N. Sakai, L. Korte, B. Rech, M.B. Johnston, L.M. Herz, H.J. Snaith, A mixed-cation lead mixed-halide perovskite absorber for tandem solar cells, Science 351 (6269) (2016) 151–155.
[65] S. Albrecht, M. Saliba, J.P. Correa Baena, F. Lang, L. Kegelmann, M. Mews, L. Steier, A. Abate, J. Rappich, L. Korte, R. Schlatmann, M.K. Nazeeruddin, A. Hagfeldt, M. Grätzel, B. Rech, Monolithic perovskite/silicon-heterojunction tandem solar cells processed at low temperature, Energy Environ. Sci. 9 (1) (2016) 81–88.
[66] J. Werner, L. Barraud, A. Walter, M. Bräuninger, F. Sahli, D. Sacchetto, N. Tétreault, B. Paviet-Salomon, S.-J. Moon, C. Allebe, M. Despeisse, S. Nicolay, S. De Wolf, B. Niesen, C. Ballif, Efficient near-infrared-transparent perovskite solar cells enabling direct comparison of 4 - terminal and monolithic perovskite/silicon tandem cells, ACS Energy Lett. 1 (2016) 474–480.

[67] C.-H. Chiang, M.K. Nazeeruddin, M. Grätzel, C.-G. Wu, The synergistic effect of H2O and DMF towards stable and 20% efficiency inverted perovskite solar cells, Energy Environ. Sci. 10 (2017) 808–817.
[68] Z. Hu, J. Miao, M. Liu, T. Yang, Y. Liang, O. Goto, H. Meng, Enhanced performance of inverted perovskite solar cells using solution-processed carboxylic potassium salt as cathode buffer layer, Org. Electron. (2017) 20.
[69] A.R. Uhl, Z. Yang, A.K.-Y. Jen, H.W. Hillhouse, Solution-processed chalcopyrite–perovskite tandem solar cells in bandgap-matched two- and four-terminal architectures, J. Mater. Chem. A Mater. Energy Sustain. 5 (7) (2017) 3214–3220.
[70] K.A. Bush, A.F. Palmstrom, Z. (Jason) Yu, M. Boccard, R. Cheacharoen, J.P. Mailoa, D.P. McMeekin, R.L.Z. Hoye, C.D. Bailie, T. Leijtens, I.M. Peters, M.C. Minichetti, N. Rolston, R. Prasanna, S.E. Sofia, D. Harwood, W. Ma, F. Moghadam, H.J. Snaith, T. Buonassisi, Z.C. Holman, S.F. Bent, M.D. McGehee, 23.6%-efficient monolithic perovskite/silicon tandem solar cells with improved stability, Nat. Energy Rev. (2017) 1–7.
[71] F. Jiang, T. Liu, B. Luo, J. Tong, F. Qin, S. Xiong, Z. Li, Y. Zhou, Two-terminal perovskite/perovskite tandem solar cell, J. Mater. Chem. A 0 (2015) 1–6.
[72] G.E. Eperon, T. Leijtens, K.A. Bush, R. Prasanna, T. Green, J.T.-W. Wang, D.P. McMeekin, G. Volonakis, R.L. Milot, R. May, A. Palmstrom, D.J. Slotcavage, R.A. Belisle, J.B. Patel, E.S. Parrott, R.J. Sutton, W. Ma, F. Moghadam, B. Conings, A. Babayigit, H.-G. Boyen, S. Bent, F. Giustino, L.M. Herz, M.B. Johnston, M.D. McGehee, H.J. Snaith, Perovskite-perovskite tandem photovoltaics with optimized band gaps, Science 354 (6314) (2016) 861–865.
[73] C.-H. Chiang, M.K. Nazeeruddin, M. Grätzel, C.-G. Wu, The synergistic effect of H2O and DMF towards stable and 20% efficiency inverted perovskite solar cells, Energy Environ. Sci. 10 (2017) 808–817.
[74] D. Zhao, Y. Yu, C. Wang, W. Liao, N. Shrestha, C.R. Grice, A.J. Cimaroli, L. Guan, R.J. Ellingson, K. Zhu, X. Zhao, R.-G. Xiong, Y. Yan, Low-bandgap mixed tin–lead iodide perovskite absorbers with long carrier lifetimes for all-perovskite tandem solar cells, Nat. Energy 2 (4) (. 2017) 17018.
[75] S. Guha, Y.S. Lee, C. Sturdevant, T.K. Todorov, Monolithic Tandem Chalcopyrite-Perovskite Photovoltaic Device. 19, 2014.
[76] A. Guchhait, H.A. Dewi, S.W. Leow, H. Wang, G. Han, F. bin Suhaimi, S.G. Mhaisalkar, L.H. Wong, N. Mathews, Over 20% efficient CIGS – perovskite tandem solar cells, ACS Energy Lett. (2017) (7b00187).
[77] F. Fu, T. Feurer, T.P. Weiss, S. Pisoni, E. Avancini, C. Andres, S. Buecheler, A.N. Tiwari, High-efficiency inverted semi-transparent planar perovskite solar cells in substrate configuration, Nat. Energy, Publ. online 19 December 2016; ⟨http://dx.doi.org/10.1038/nenergy.2016.190⟩, vol. 2, no. December, 2016, pp. 1234–1237.
[78] Y.S. Lee, M.T. Winkler, S.C. Siah, R. Brandt, T. Buonassisi, Hall mobility of cuprous oxide thin films deposited by reactive direct-current magnetron sputtering, Appl. Phys. Lett. 98 (19) (2011) 1–4.
[79] C. Xiang, G.M. Kimball, R.L. Grimm, B.S. Brunschwig, H. a. Atwater, N.S. Lewis, 820 mV open-circuit voltages from Cu2O/CH3CN junctions, Energy Environ. Sci 4 (2011) 1311.
[80] Y.S. Lee, J. Heo, S.C. Siah, J.P. Mailoa, R.E. Brandt, S.B. Kim, R.G. Gordon, T. Buonassisi, Ultrathin amorphous zinc-tin-oxide buffer layer for enhancing heterojunction interface quality in metal-oxide solar cells, Energy Environ. Sci. 6 (7) (2013) 2112–2118.
[81] S. Eisermann, A. Kronenberger, A. Laufer, J. Bieber, G. Haas, S. Lautenschläger, G. Homm, P.J. Klar, B.K. Meyer, Copper oxide thin films by chemical vapor deposition: synthesis, characterization and electrical properties, Phys. Status Solidi A 209 (3) (2012) 531–536.
[82] Y.S. Lee, J. Heo, S.C. Siah, J.P. Mailoa, R.E. Brandt, S.B. Kim, R.G. Gordon, T. Buonassisi, Ultrathin amorphous zinc-tin-oxide buffer layer for enhancing heterojunction interface quality in metal-oxide solar cells, Energy Environ. Sci. 6 (7) (2013) 2112–2118.
[83] Y.S. Lee, D. Chua, R.E. Brandt, S.C. Siah, J.V. Li, J.P. Mailoa, S.W. Lee, R.G. Gordon, T. Buonassisi, Atomic layer deposited gallium oxide buffer layer enables 1.2 V open-circuit voltage in cuprous oxide solar cells, Adv. Mater. 26 (27) (2014) 4704–4710.
[84] M. Tadatsugu, N. Yuki, M. Toshihiro, Efficiency enhancement using a $Zn_{1-x}Ge_x$-O thin film as an n-type window layer in Cu_2O-based heterojunction solar cells, Appl. Phys. Express 9 (5) (2016) 52301.
[85] M. Tadatsugu, N. Yuki, M. Toshihiro, Efficiency enhancement using a $Zn_{1-x}Ge_x$-O thin film as an n-type window layer in Cu_2O-based heterojunction solar cells, Appl. Phys. Express 9 (5) (2016) 52301.
[86] T.K. Todorov, S. Singh, D.M. Bishop, Y.S. Lee, T.S. Gershon, P.D. Antunez, R.A. Haight, Ultrathin, record-performance solar cells with high band gap from the world's oldest photovoltaic material, Nat. Commun., 2017.